J Electroceram (2009) 22:98–104
DOI 10.1007/s10832-008-9491-5

Microstructure and luminescent properties of $Eu_2W_2O_9$ phosphors

Kyung-Hoon Cho · Kyoung-Pyo Hong · Sahn Nahm · Bo-Yun Jang · Joo-Seok Park · Soon-Jae Yoo

Received: 13 April 2007 / Accepted: 19 March 2008 / Published online: 13 April 2008

Abstract A homogeneous $Eu_2W_2O_9$ phase with small grains (~4.0μm) was formed for the specimens fired below 1175°C. As the firing temperature was increased above 1150°C, grain growth occurred and the grain shape changed from faceted to round. The excitation spectra of the $Eu_2W_2O_9$ phosphor were similar to those of the $Eu_2(WO_4)_3$ phosphor, but the absorption band due to the $O^{2-} \rightarrow W^{6+}$ ligand to metal charge transfer was shifted to lower energies and the $^7F_o \rightarrow {}^5H_3$ and $^7F_o \rightarrow {}^5F_{2,4}$ transitions were not found. The intensity of the excitation and emission spectra of the $Eu_2W_2O_9$ phosphor considerably increased with increasing firing temperature, due to the increased grain size and changed grain shape. The intensity of the red emission band of the $Eu_2W_2O_9$ phosphor was higher than that of the $Eu_2(WO_4)_3$ phosphor. Moreover, the addition of LiCl to the $Eu_2W_2O_9$ phosphors considerably enhanced the intensity of their emission spectra, probably due to the increased grain size. Therefore, LiCl-added, $Eu_2W_2O_9$ phosphor is a promising candidate material for red color emission.

K.-H. Cho · K.-P. Hong · S. Nahm (✉)
Department of Materials Science and Engineering,
Korea University,
5 Ga Anam-Dong, Sungbuk-Gu,
Seoul 136-701, South Korea
e-mail: snahm@korea.ac.kr

B.-Y. Jang · J.-S. Park
Korea Institute of Energy Research,
71-2 Jang-Dong, Yoosung-Gu,
Daejon 305-343, South Korea

S.-J. Yoo
Itswell Co., Ltd,
9-4BL, Ochang Scientific Industrial Complex, 1115-4,
Namchon-ri, Oksan-myeon, Cheongwon-gun,
Chungbuk 363-911, South Korea

Keywords Red phosphor · $Eu_2W_2O_9$ · Photo-luminescence · Microstructure

1 Introduction

Recently, white light based on the ultraviolet light-emitting diode (UV-LED) combined with phosphors has been intensively investigated [1]. A blue LED with the YAG: Ce^{3+} phosphor was produced by the Nichia Co. [2]. However, this system showed a poor color rendering index (CRI) caused by the lack of red color and a halo effect due to the separation of the blue and yellow colors [3]. High quality white light can be obtained by using a UV-LED with red, green and blue phosphors [4, 5]. However, it is very difficult to make a red phosphor with a high intensity which is excited in the wavelength range of 380~410nm. Many investigations have been conducted to produce red phosphors, such as $Sr_2P_2O_7$:Eu^{2+}, Mn^{2+} and $(Y_{1.9}Eu_{0.1})O_3$ [6, 7]. However, their intensity was very low compared with that of the blue and green phosphors, making it difficult to generate white light with high performance. Solid solutions containing Eu^{3+} ions such as $CsEuW_2O_8$ and $AgEuW_2O_8$ have been studied for red emission phosphors, because the Eu^{3+} ion has an absorption band at around 395nm with a red emission and concentration quenching was not observed in these solid solutions [8–10]. The luminescent properties of $Na_9(EuW_{10}O_{36})\cdot 14H_2O$ polyoxometalate and $[EuW_{10}O_{36}]^{9-}$ were also investigated [11–13]. In particular, the promising luminance properties exhibited by $Eu_2(WO_4)_3$ phosphor have led it to be well investigated [14, 15]. In contrast, the $Eu_2W_2O_9$ phosphor has attracted very little systematic investigation.

In this work, the variations of the microstructure and luminescent properties of the $Eu_2W_2O_9$ phosphor according

to various process conditions were systematically investigated and compared with those of the $Eu_2(WO_4)_3$ phosphor. In addition, LiCl was added to enhance the intensity of the red emission of the $Eu_2W_2O_9$ phosphor.

2 Experimental details

Eu_2O_3 (99.99%, Aldrich), WO_3 (99.99%, Aldrich), and LiCl (99.99%, Aldrich) were used as starting materials to prepare the $Eu_2W_2O_9$, $Eu_2(WO_4)_3$ and LiCl-added $Eu_2W_2O_9$ phosphors. They were mixed and ground for 2 h in an agate mortar using acetone and then dried. The dried powders were fired at 1000~1200°C for 2 h in alumina crucibles. The structural properties of the specimens were examined by X-ray diffraction (XRD: Rigaku D/max-RC) and scanning electron microscopy (SEM: Hitachi S-4300, Japan). The photo-luminescence (PL) excitation and emission spectra were obtained using an Aminco–Bowman luminescence spectrometer with a xenon-lamp as a light source. To obtain a qualitative comparison between the emission and excitation intensities of the different spectra, measurements were conducted consecutively and all the experimental conditions such as the optical set up, focalization point and illuminated cross-section, the sample holder and emission and excitation slit width (0.4 mm), were kept constant. Moreover, approximately the same amount of sample was used for the measurements in each case. In addition, for the precise measurement of the emission and excitation spectra, an instrumental correction was made for the detection/optical response and spectral distribution of the lamp. In particular, the correction for the spectral distribution of the lamp was carried out by measuring the bare intensity of the light source using a reference detector. For the excitation spectra measurements, the emission was monitored at the wavelength of the maximum intensity in the emission spectra and the excitation wavelength was scanned from 250 to 500 nm. The excitation wavelength of the maximum intensity was fixed during the emission spectra measurements. For the measurement of the radiant efficiency of the phosphors, a bullet type LED lamp consisting of a UV-LED chip (λ = 405 nm, Itswell Co. Korea) and transparent Si resin, was fabricated. The radiant efficiency and Commission International de l'Eclairage (CIE, France, 1931) chromaticity coordinates of the phosphors were measured by a spectrometer (Lapsphere, CDS1100) with a 10-in. diameter integrated sphere.

3 Results and discussion

Figure 1 shows the XRD patterns of the $Eu_2W_2O_9$ phosphors fired at various temperatures. For the specimens fired between 1125°C and 1175°C, a homogeneous monoclinic $Eu_2W_2O_9$ phase with the $P2_1/c$ space group was formed. As the firing temperature was increased above 1175°C, peaks for the $Eu_2(WO_4)_3$ second phase, indicated by the arrows, appeared and the specimens started to melt when the firing temperature exceeded 1250°C. Since the Eu_2O_3 evaporated at a temperature close to the melting temperature of $Eu_2W_2O_9$ and no second phase related to the

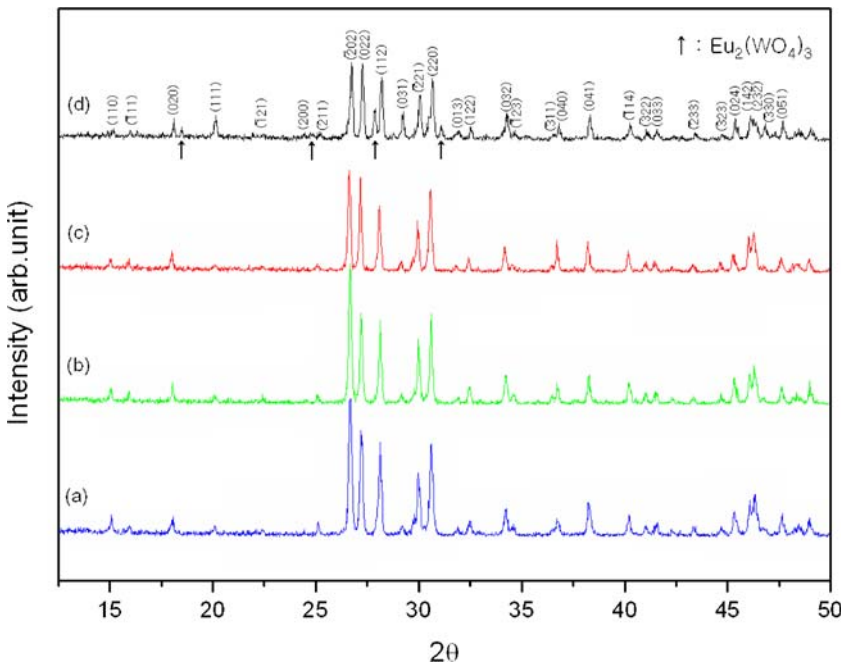

Fig. 1 XRD patterns of the $Eu_2W_2O_9$ phosphor fired at various temperatures: (**a**) 1125°C, (**b**) 1150°C, (**c**) 1175°C and (**d**) 1200°C

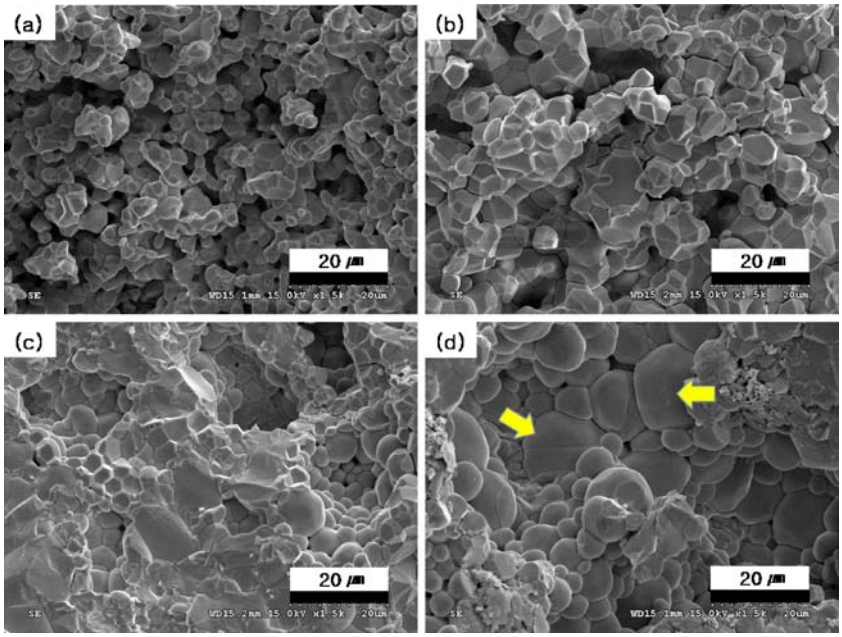

Fig. 2 SEM images of the $Eu_2W_2O_9$ phosphors fired at various temperatures: (**a**) 1125°C, (**b**) 1150°C, (**c**) 1175°C and (**d**) 1200°C

tungsten oxide was observed in this specimen, the formation of the $Eu_2(WO_4)_3$ second phase may have been caused by the evaporation of the Eu_2O_3 during the firing at 1200°C.

The microstructure of the $Eu_2W_2O_9$ specimens fired at various temperatures was investigated using SEM, as shown in Fig. 2(a)–(d). For the specimens fired below 1175°C, faceted small grains with an average grain size of ~4.0 μm were formed, as shown in Fig. 2(a) and (b). Grain growth occurred as the firing temperature was increased above 1150°C and some of the grains indicated by arrows had a large grain size of ~20 μm. Furthermore, the shape of the grain started to change from faceted to round at 1175°C and round-shaped grains were formed in the specimen fired at 1200°C.

The excitation spectra of the $Eu_2W_2O_9$ phosphors fired at various temperatures were obtained in the spectral ranges from 250 to 500 nm under emission at 614 nm, as shown in Fig. 3(a). The intensity of all of the peaks increased with increasing firing temperature, probably due to the increased grain size. Furthermore, the change in the grain shape from faceted to round was also considered to have contributed to

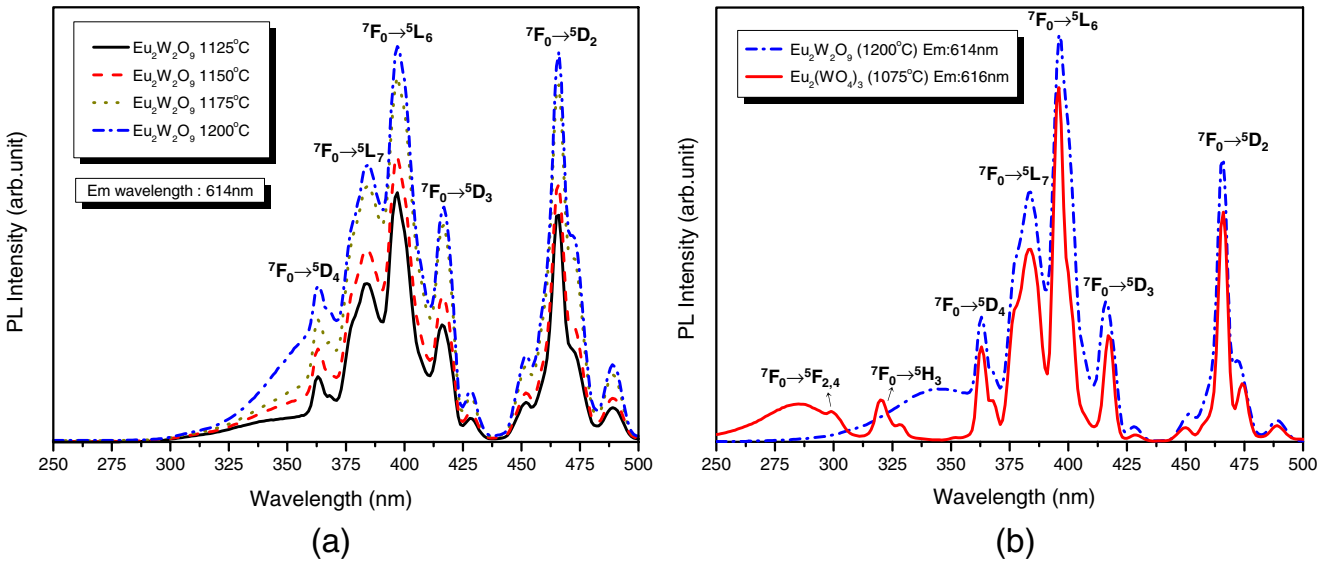

Fig. 3 Excitation spectra of (**a**) $Eu_2W_2O_9$ phosphors (λ_{em}=614 nm) fired at various temperatures and of (**b**) $Eu_2W_2O_9$ (λ_{em}=614 nm) and $Eu_2(WO_4)_3$ phosphors (λ_{em}=616 nm) fired at 1200°C and 1075°C, respectively

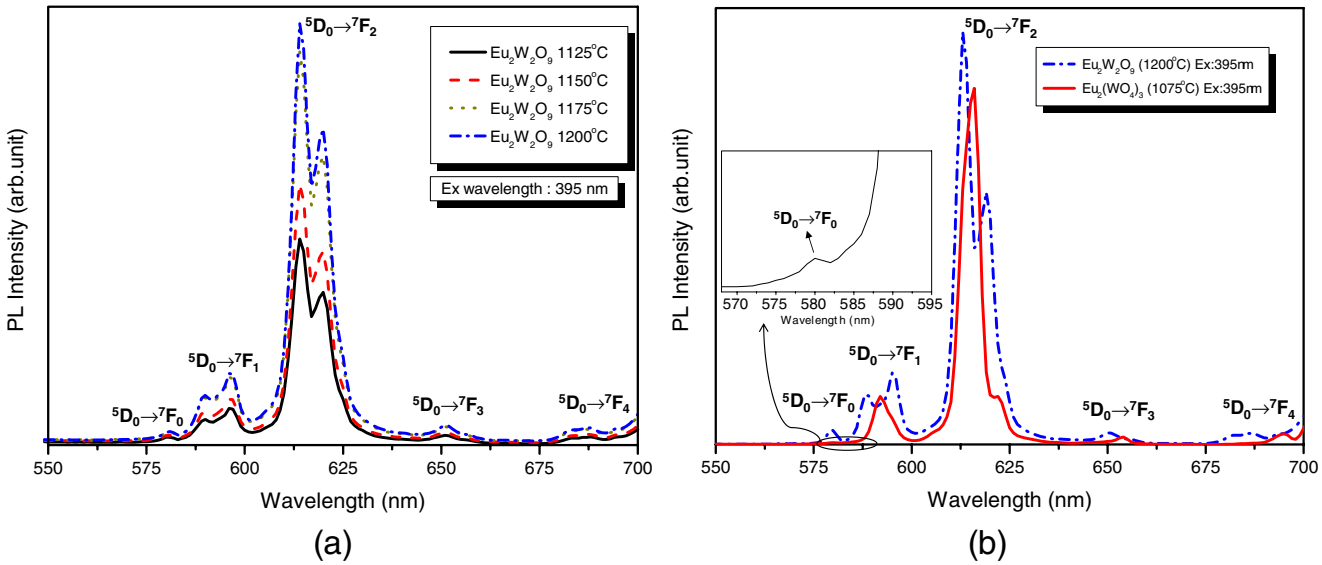

Fig. 4 Emission spectra of (**a**) $Eu_2W_2O_9$ phosphors fired at various temperatures and of (**b**) $Eu_2W_2O_9$ and $Eu_2(WO_4)_3$ phosphors fired at 1200°C and 1075°C, respectively. (λ_{ex}=395 nm)

the increased PL intensity, because the efficiency of the absorption increased for the round-shaped particles. The excitation spectra of the $Eu_2(WO_4)_3$ phosphors were also obtained and compared with those of $Eu_2W_2O_9$, as shown in Fig. 3(b). The excitation spectra of two specimens were similar, consisting of two sharp lines at 395 and 465 nm corresponding to the $^7F_o \rightarrow ^5L_6$ and $^7F_o \rightarrow ^5D_2$ transitions of the Eu^{3+} ion, respectively. However, the $^7F_o \rightarrow ^5H_3$ and $^7F_o \rightarrow ^5F_{2,4}$ transitions, which were found in the $Eu_2(WO_4)_3$ phosphor, were not observed in the $Eu_2W_2O_9$ phosphor, probably due to the different crystal structure. The broad peak at around 260~310 nm, which was observed in the $Eu_2(WO_4)_3$ phosphor due to $O^{2-} \rightarrow W^{6+}$ ligand to metal charge transfer (LMCT), was not found in the $Eu_2W_2O_9$ specimen, but a broad peak was observed at around 300~425 nm. The $P2_1/c$ space group of the $E_2W_2O_9$ phase contains a WO_6 unit, and the $Eu_2(WO_4)_3$ phase with the C2/c space group has a WO_4 unit. G. Blasse suggested that the absorption transition due to $O^{2-} \rightarrow W^{6+}$ LMCT is shifted to lower energies with increasing number of ligands [16]. Therefore, the broad peak at around 300~425 nm in the $Eu_2W_2O_9$ phase was considered to be due to the $O^{2-} \rightarrow W^{6+}$ LMCT of the WO_6 unit. Furthermore, since the $O^{2-} \rightarrow Eu^{3+}$ LMCT occurred at around 310 nm, this broad peak at

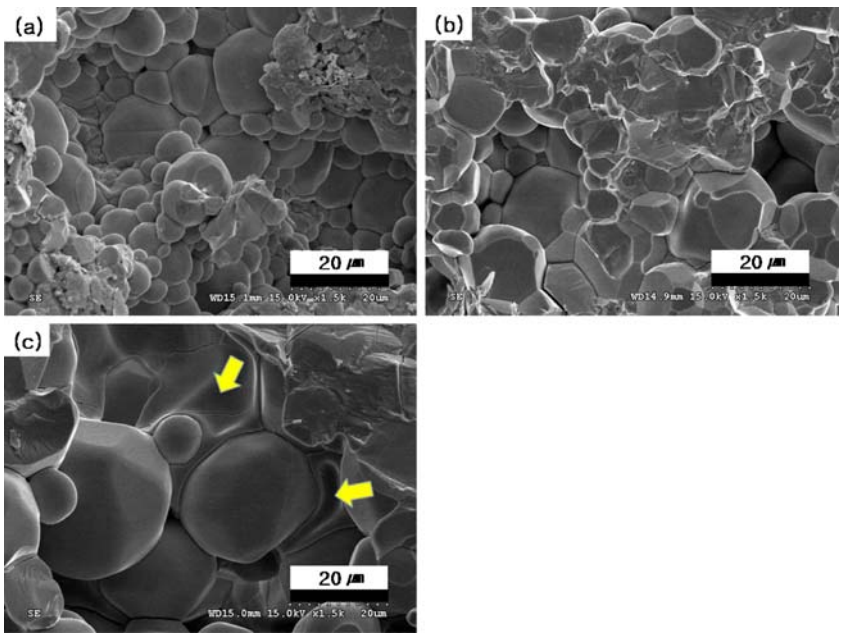

Fig. 5 SEM images of $Eu_2W_2O_9$+x mol% LiCl phosphors fired at 1200°C: (**a**) x=0.0, (**b**) x=3.0 and (**c**) x=10.0

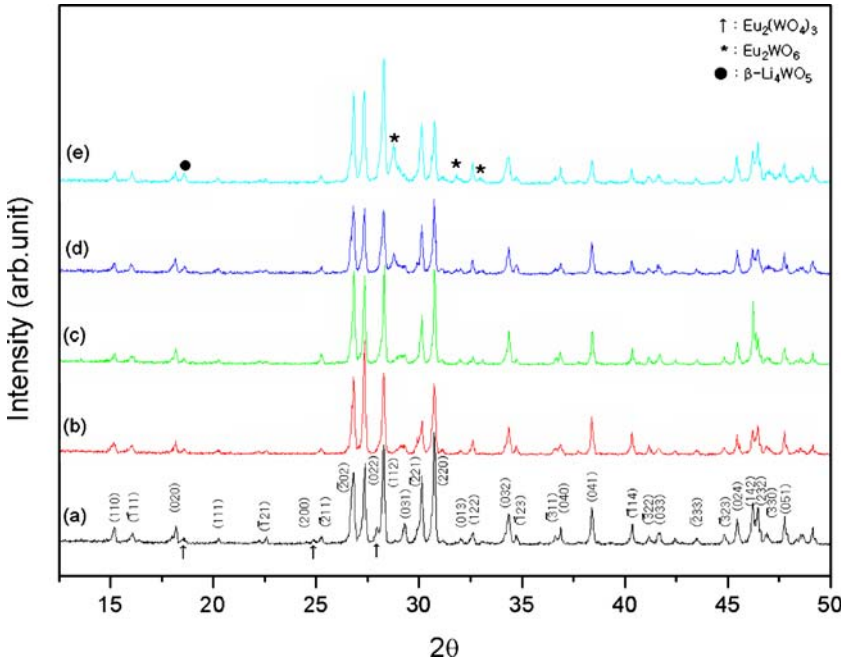

Fig. 6 XRD patterns of $Eu_2W_2O_9$+x mol% LiCl phosphors fired at 1200°C: (**a**) x=1.0, (**b**) x=3.0, (**c**) x=5.0, (**d**) x=7.0 and (**e**) x=10.0

around 300~425 nm was attributed to both the $O^{2-}\rightarrow W^{6+}$ and $O^{2-}\rightarrow Eu^{3+}$ LMCT transitions. In addition, the contribution of the LMCT band absorption to the excitation spectra was lower than that of the absorption lines of the Eu^{3+} ion, indicating that the energy absorption at 395 nm was almost via the intra-$4f^6$ levels of the Eu^{3+} ion, rather than the sensitization via LMCT. This line absorption of the Eu^{3+} ion and very small contribution of the LMCT band can limit the efficiency of this phosphor under low excitation energy (λ = 395 nm).

The emission spectra of the $Eu_2W_2O_9$ phosphors fired at various temperatures were obtained under excitation at 395 nm, as shown in Fig. 4(a). The intensity of the emission peak increased with increasing firing temperature, probably due to the increased grain size and rounded grain shape. The emission spectra of the $Eu_2(WO_4)_3$ phosphor were also measured and the comparison with those of the $Eu_2W_2O_9$ specimens revealed them to be very similar, with five bands assigned to the $^5D_o\rightarrow{}^7F_J$ (J = 0,1,2,3,4) transitions, as shown in Fig. 4(b). However, the intensity of the emission of the $^5D_o\rightarrow{}^7F_0$ transition for the $Eu_2(WO_4)_3$ phosphor was very weak compared with that of the $Eu_2W_2O_9$ phosphor. Furthermore, two emission peaks were observed for the $^5D_o\rightarrow{}^7F_1$ transition in the case of the $Eu_2W_2O_9$ phosphor,

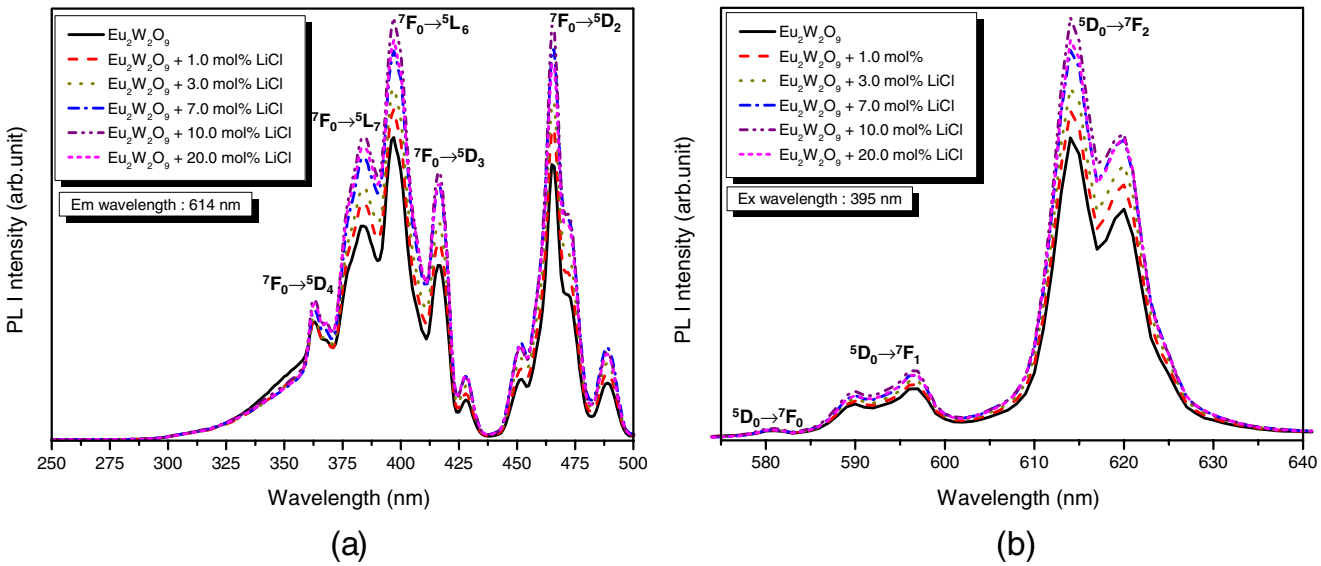

Fig. 7 (**a**) Excitation (λ_{em}=614 nm) and (**b**) emission (λ_{ex}=395 nm) spectra of $Eu_2W_2O_9$+x mol% LiCl phosphors with 0.0≤x≤20.0 fired at 1200°C

Table 1 Radiant efficiencies of the UV-LED lamps which consisted of the $Eu_2W_2O_9$+10.0 mol% LiCl phosphor and Si resin.

Phosphor: Si	405 nm output (Pc) from the LED chip (mW)	614 nm output (Pp) from the phosphor (mW)	Radiant efficiency (Pp/(Pb−Pc))
5:95	9.59	0.15	0.21
10:90	8.97	0.29	0.22
15:85	8.72	0.37	0.23

Original power of bare LED chip (Pb): 10.3 mW

but only one for the $Eu_2(WO_4)_3$ phosphor. These differences could be explained by the difference in the crystal field due to the different crystal structure. In addition, the intensity of the $^5D_o \rightarrow {}^7F_2$ transition peak at around 614 nm was higher for the $Eu_2W_2O_9$ phosphor than for the $Eu_2(WO_4)_3$ phosphor.

LiCl additive, which has a low melting temperature of 605°C, was used to assist the formation of the $Eu_2W_2O_9$ phase and grain growth, because the intensity of the emission peaks of the $Eu_2W_2O_9$ phase increased with increasing grain size. Figure 5(a)–(c) show the SEM images of the $Eu_2W_2O_9$ + *x*mol% LiCl specimens with $0.0 \leq x \leq 10.0$ fired at 1200°C. The average grain size increased significantly with increasing LiCl content, reaching approximately 25~30 μm in the 10.0 mol% LiCl-added specimen. This increase in the grain size was explained by the presence of the liquid phase in the 10.0 mol% LiCl-added specimen, as indicated by the arrows in Fig. 5(c). According to the phase diagram, Li_2O and WO_3 have a eutectic point at 665°C, indicating that the liquid phase could be a Li_2O–WO_3 related phase. [17]

Figure 6 shows the XRD patterns of the $Eu_2W_2O_9$ + *x*mol% LiCl phosphors with $1.0 \leq x \leq 10.0$. All the specimens had the $Eu_2W_2O_9$ phase. However, the amount of the $Eu_2(WO_4)_3$ second phase found in the $Eu_2W_2O_9$ specimen fired at 1200°C decreased with increasing LiCl content and disappeared at $x > 3.0$ mol%. Moreover, peaks for the Eu_2WO_6 and β-Li_4WO_5 second phases, indicated by the asterisks and full circle, respectively, appeared when the LiCl content exceeded 5.0 mol%. Since some of the Eu_2O_3 evaporated during the firing at 1200°C, Li_2O was considered to have reacted with the tungsten oxide forming the Li_2O–WO_3 related liquid phase and the $Eu_2W_2O_9$ phase changed to the Eu_2WO_6 second phase instead of $Eu_2(WO_4)_3$. Furthermore, β-Li_4WO_5 phase was considered to be formed from the liquid phase during cooling.

Figure 7(a) and (b) show the excitation and emission spectra of the $Eu_2W_2O_9$ + *x*mol% LiCl phosphors with $0.0 \leq x \leq 20.0$. The shape of the excitation and emission spectra did not change, but their intensity significantly increased with increasing LiCl content up to 10.0 mol%. However, their intensity subsequently decreased, possibly due to the increased amount of second and liquid phases.

In order to evaluate its quantitative luminescent properties and demonstrate the possibility of using it as a red phosphor for UV-LEDs, the $Eu_2W_2O_9$ + 10.0 mol% LiCl phosphor powder was packaged in a UV-LED chip. The radiant efficiency of this phosphor, which is defined as the ratio of the emitted luminescent power to the absorbed power, was measured and the results are summarized in Table 1. The radiant efficiency increased with increasing amount of the phosphor, but not significantly, remaining approximately 22%. Generally, the radiant efficiency of a

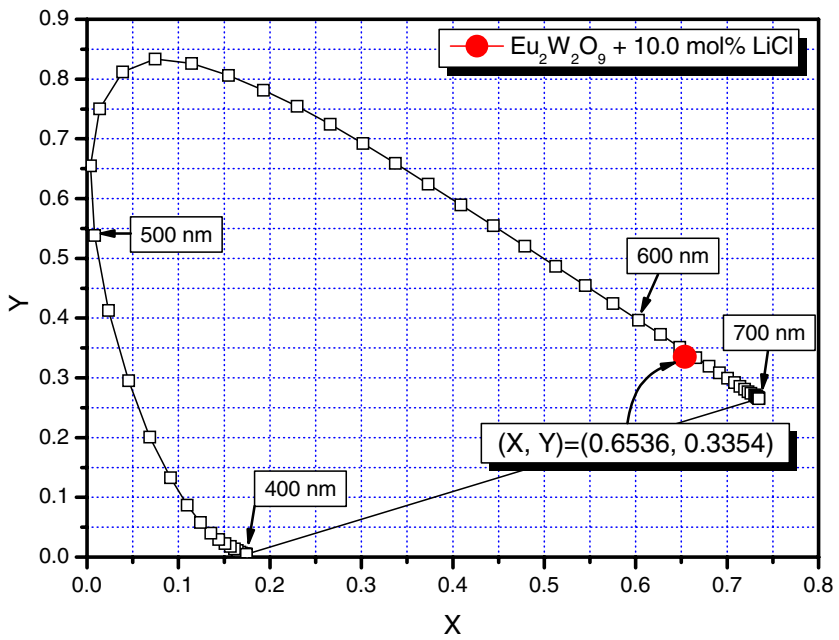

Fig. 8 The CIE chromaticity coordinates of the PL of the $Eu_2W_2O_9$+10.0 mol% LiCl phosphor

phosphor is lower than the quantum efficiency, due to the energy loss in the device. However, the radiant efficiency of the 10.0mol% LiCl added $Eu_2W_2O_9$ phosphor (22%) is higher than the quantum efficiency of the $Eu_2(WO_4)_3$ phosphor [14]. Therefore, the 10.0mol% LiCl added $Eu_2W_2O_9$ has the potential to be used as a red phosphor.

Figure 8 shows the CIE chromaticity coordinates of the PL of the $Eu_2W_2O_9$+10.0 mol% LiCl phosphor. They are x=0.65 and y=0.33, indicating that the chromaticity coordinates of this phosphor are very good for a red phosphor and are comparable to those of the $K_5Eu_2(WO_4)_{5.5}$ (x=0.63, y=0.35) and Y_2O_2S:Eu (x=0.64, y=0.34) phosphors [18].

4 Conclusions

A homogeneous $Eu_2W_2O_9$ phase with small grains (~4.0 μm) was formed for the phosphors fired below 1175°C. As the firing temperature was increased above 1150°C, grain growth occurred and the grain shape changed from faceted to round. $Eu_2(WO_4)_3$ second phase was observed in the specimen fired at 1200°C due to the evaporation of Eu_2O_3 during the firing. The intensity of the excitation and emission spectra of the $Eu_2W_2O_9$ phosphor considerably increased with increasing firing temperature, probably due to the increased grain size and changed grain shape. The intensity of the red emission peak at around 614 nm was higher for the $Eu_2W_2O_9$ phosphor than for the $Eu_2(WO_4)_3$ phosphor. To enhance the intensity of the red emission of the $Eu_2W_2O_9$ phosphor by increasing the grain size of the powders, LiCl was added. The addition of LiCl did not alter the shape of the excitation and emission spectra, but their intensity was considerably increased due to the increased grain size. Therefore, LiCl-added $Eu_2W_2O_9$ phosphor can be a promising candidate material for red color emission.

Acknowledgement This work was supported by a Korea Energy Management Corporation Grant (2005-E-FM11-P-11-3-030-2006).

References

1. S. Nakamura, T. Mukai, M. Senoh, J. Appl. Phys. **76**, 8189 (1994) DOI 10.1063/1.357872
2. R. Muller-Mach, G.O. Mueller, IEEE J. Sel. Top. Quantum Electron. **8**, 339 (2002) DOI 10.1109/2944.999189
3. V. Sivakumar, U.V. Varadaraju, J. Electrochem. Soc. **154**(1), J28 (2007) DOI 10.1149/1.2382266
4. A.M. Srivastava, H.A. Comanzo, U.S. Pat. No. 6,501,100 (2002)
5. T. Matsuda, A. Aruga, K. Shioi, J. Alloys Compd. **408–412**, 852 (2006) DOI 10.1016/j.jallcom.2004.12.100
6. A.M. Srivastava, H.A. Comanzo, T.F. McNulty, U.S. Pat. No. 6,621,211 B1 (2003)
7. C.Y. Wang, R.S. Liu, Y.S. Lin, C.C. Kang, L.S. Chi, H. Y. Su, H. C. Chen-Lun, U.S. Pat. No. 6,805,600 B2 (2004)
8. C.C. Torardi, C. Page, L.H. Brixner, G. Blasse, G.J. Dirksen, J. Solid State Chem. **69**, 171 (1987) DOI 10.1016/0022-4596(87)90023-5
9. F. Shi, J. Meng, Y. Ren, Q. Su, J. Phys. Chem. Solids **59**(1), 105 (1997) DOI 10.1016/S0022-3697(97)00148-0
10. F. Shi, J. Meng, Y. Ren, Q. Su, J. Mater. Chem. **7**(5), 773 (1997) DOI 10.1039/a607241k
11. R.A. Sa Ferreira, S.S. Nobre, C.M. Granadeiro, H.I.S. Nogueira, L.D. Carlos, O.L. Malta, J. Lumin. **121**, 561 (2003) DOI 10.1016/j.jlumin.2005.12.044
12. R. Ballardini, Q.G. Mulazzani, M. Venturi, F. Bolletta, V. Balzani, Inorg. Chem. **23**, 300 (1984) DOI 10.1021/ic00171a007
13. F.L. Sousa, M. Pillinger, R.A. Sa Ferreira, C.M. Granadeiro, A.M. V. Cavaleiro, J. Rocha, L.D. Carlos, T. Trindade, H.I.S. Nogueira, Eur. J. Inorg. Chem. **2006**, 726 (2006) DOI 10.1002/ejic.200500518
14. C.A. Kodaira, H.F. Brito, O.L. Malta, O.A. Serra, J. Lumin. **101**, 11 (2003) DOI 10.1016/S0022-2313(02)00384-8
15. C.A. Kodaira, H.F. Brito, M.C.F.C. Felinto, J. Solid State Chem. **171**, 401 (2003) DOI 10.1016/S0022-4596(02)00221-9
16. G. Blasse, B.C. Grabmaier, Luminescent materials (Springer, Berlin, 1994)
17. J. Hauck, J. Inorg. Nucl. Chem. **36**(10), 2291 (1974) DOI 10.1016/0022-1902(74)80272-1
18. Y.R. Do, Y.D. Huh, J. Electrochem. Soc. **47**(11), 4385 (2000) DOI 10.1149/1.1394074